Model calculations of polarization-dependent two-color high-harmonic generation

S. Long, W. Becker,* and J. K. McIver
Center for Advanced Studies, Department of Physics and Astronomy, University of New Mexico, Albuquerque, New Mexico 87131
(Received 3 April 1995)

Emission rates for high-harmonic generation by a zero-range-potential model atom in the superposition of two monochromatic plane-wave fields are calculated. Several polarizations of the driving fields are considered: two linear polarizations enclosing an arbitrary angle, and two circularly polarized fields that co- or counter-rotate in the same plane. Transition amplitudes are obtained in the form of sums of one-dimensional integrals that have to be computed numerically. For commensurate frequencies of the driving fields the results depend critically on the relative phase between the two fields. Parallel driving fields are not always more efficient in harmonic generation than perpendicular fields; also, two circular polarizations can be at least as effective. The odd harmonics of one field are usually weakened by the addition of the other field in favor of the mixed harmonics. If the ratio of the frequencies of the two incident fields equals the ratio of two odd integers, then harmonics with elliptic polarization can be generated by two linearly polarized driving fields. Harmonics with circular polarization can readily be produced with the help of two incident circularly polarized fields whose field vectors co-rotate or counter-rotate in the same plane.

PACS number(s): 32.80.Rm, 42.65.Ky

I. INTRODUCTION

The first experiments on the generation of very high harmonics by an intense laser field irradiating a gaseous target [1] have set off a major collaborative effort of experimentalists and theorists in order to elucidate the underlying physical mechanisms. Owing to its nonperturbative character as expressed, e.g., in the existence of the "plateau" high-harmonic generation (HHG) holds great intrinsic interest. However, the potential of practical applications as a source of bright coherent light with a choice of polarization characteristics is no less important, particularly, since it leads into a frequency regime where few other sources are available.

The process of HHG as observed experimentally has both single-atom and collective aspects: the emission of a high-harmonic photon by some individual atom on the one hand as well as the ensuing propagation in the gas and the superposition of radiation emitted by different atoms on the other. The collective aspects can be dealt with classically and are now well understood [2]. They will not be considered in this paper. The single-atom aspect is calculated either by a numerical solution of the time-dependent Schrödinger equation or by more or less detailed modeling. To date, the most extensive theoretical treatments include both aspects and have yielded good agreement with the data [3]. A semiclassical approach [4,5] to the single-atom aspects has met with remarkable success in providing intuitive understanding of the physical mechanism and also describing the data at least semiquantitatively: the atom is assumed to release an electron into the continuum with near zero velocity, either via tunneling or multiphoton ionization. Subsequently, the electron is accelerated by the field. Depending on the time it appeared in the continuum it may revisit the ionic core and recombine leading to the quantum mechanical event of HHG. In this simplest version the model is obviously restricted to a linearly polarized laser field, since otherwise the electron will never revisit the core.

Up to now most experimental as well as theoretical work has concentrated on HHG by one monochromatic linearly polarized laser field. There are, however, measurements of HHG by a monochromatic elliptically polarized field, concentrating on the rates of harmonic emission [6,7] or on the rotation of the axis of the ellipse of polarization of the emitted harmonics as compared to that of the incident field [8]. There are a few experimental investigations of two-color HHG, for the case where one field is the second harmonic of the other and the two fields are of very different [9] or comparable [10] magnitude. Moreover, results have been published for a frequency ratio of 3:1 [11]. In all of these experiments, the frequencies of the two fields have been commensurate so that the relative phase is physically well defined. However, it appears that in all of these cases the experiment was not able to control the phase. Since this is experimentally possible by now [8,11], the situation is likely to change soon. As for theory, at the time of this writing we are only aware of one paper [12] that touches upon two-color HHG.

High-harmonic generation by a two-color laser field has a huge parameter space: the intensities of the two fields, their polarizations, their frequency ratio, and, if commensurate, their relative phase can be varied. The

*Also at Physik Department T30, Technische Universität München, D-85747 Garching, Germany.

calculations to be presented in this paper will demonstrate that the characteristics of the high-harmonic emission may dramatically depend on these parameters. There is some hope that this can be exploited for tailoring the harmonic output to ones liking. For example, one may think of extending the plateau, suppressing or enhancing particular harmonics or entire frequency regions, quenching ionization and thereby increasing the saturation intensity, or generating particular polarizations, such as getting circular polarization out of incident linear polarizations. If, in the commensurate case, a certain combination of the phases of the two fields can be controlled, this offers a particularly efficient way of manipulating the harmonic emission rates relative to each other. There is a close correspondence to "coherent control" in photochemistry, i.e., controlling the branching ratios into different reaction channels by varying the relative phase between the laser fields [13]. Conversely, once this is understood it can be used to measure the relative phase between two laser fields [14].

Trying, however, to find the appropriate values of the parameters for a given objective by means of a shotgun approach, either experimentally or theoretically, appears as promising as searching for the famous needle in the haystack. What is needed is some guide to the regions of the parameter space which are most appropriate for a given purpose. A suitable generalization of the aforementioned semiclassical model may turn out to serve as such. As it stands, however, there is the problem that for all but linearly polarized fields a classical electron released with zero velocity does not return to the site of its release. There are several ways in which the semiclassical model [4,5] may nevertheless be extended to deal with general polarizations: (i) due to the finite range of a realistic binding potential the electron only needs to return to within the range of the potential; (ii) quantum-mechanical wave-packet spreading ensures that the classical trajectory of the electron needs not to return to the exact site of release [5]; and (iii) nonzero initial velocities may be important [15]. Of these, the first possibility is trivial. It will certainly contribute to HHG in a finite-range potential. The second is invariably part of any fully quantum-mechanical description. The third becomes apparent if one considers the path-integral representation of the electron propagator in an external field. It has been shown that the classical electron orbits which have the electron return with maximal kinetic energy are such that initial and final velocities are perpendicular [15]. Only for linearly polarized laser fields does this allow for an initial velocity of zero. In this paper we will not attempt to identify such a generalized semiclassical model that is capable of dealing with polarizations that are not linear. Rather, we will pursue the more modest goal of providing compact expressions for the various two-color high-harmonic emission rates as well as their polarizations in the form of one-dimensional integrals that allow for a comparatively quick numerical evaluation.

As opposed to HHG, there is a very substantial amount of work on multiphoton ionization by two fields, mostly theoretical. In particular, two configurations have been investigated: the combination of a low-intensity high-frequency field and a high-intensity low-frequency field [16] or, alternatively, two fields with commensurate frequencies so that the relative phase does matter [17,18]. This has been done with various motivations. Here we just mention that the first case has been used as a testing ground for the impact of the ponderomotive barrier (created predominantly by the high-intensity low-frequency field) on total and partial ionization rates while the second situation allows for the study of the influence of the relative phase on the same quantities and of the effects of interference and resonances, the latter being most pronounced for a frequency ratio of 3:1 [18]. Experiments have been directed at the first case with the ponderomotive potential in mind [19] and the second in order to study the effect of the relative phase on the above-threshold ionization spectra [11,20].

In this paper, we will model two-color HHG by replacing the atomic binding potential by a zero-range potential [21,22]. In particular, we will refer to our earlier paper [22] which deals with HHG by one monochromatic laser field of arbitrary polarization as I. The model is closely related to the description of Ref. [23] which satisfies all the same model assumptions that we will make here. The zero-range potential has, in general, fared quite well in reproducing qualitative trends of the data. For one-color HHG, it has been used by several groups for fits and interpretations of their experimental results [24–26]. In particular, it was employed in order to decide whether or not measured harmonic signals were due to the atom or the ion [26]. For HHG by a one-color field with elliptical polarization we have obtained in I a satisfactory description of the data of Ref. [6]. Expressions specifying the rotation of the axis of the polarization ellipse of the emitted harmonic radiation versus that of the incident field can also be found in I, but have not yet been evaluated numerically for a comparison with the recent experimental results [8]. The results of this paper have already been compared to the results of an experimental study of two-color high-harmonic emission for a frequency ratio of 2:1 for various polarizations of the incident fields [10]. Generally, the agreement was good.

The layout of the paper is as follows. In the second section, we derive expressions for the emission rates of two-color harmonics for several polarization configurations of the driving fields. The formalism that we use is a rather straightforward extension of the earlier methods used in I, and we will frequently refer to this paper. However, all of the nomenclature is explained in the present paper, too. In all cases, the resulting transition amplitudes have the form of one-dimensional quadratures which are very similar to those encountered in I. The calculation of the emission rate for a given two-color harmonic is more time consuming than in the one-color case, however, since many of these integrals have to be summed over. We present formulas for two linearly polarized incident fields which may enclose an arbitrary angle, and, in particular, for two perpendicular polarizations where the expressions assume their simplest form. If the frequencies of the incident fields are commensurate, a given harmonic frequency can be reached via different pathways and all of the corresponding transition ampli-

tudes must be summed up before the transition rate is evaluated. Specifically, we write down explicit results for a 2:1 frequency ratio. Another polarization configuration that we investigate extensively is the case of two circular polarizations which are co-rotating or counter-rotating in the same place. The emitted spectrum consists of comparatively few lines in this case, owing to particularly simple angular momentum selection rules. With the exception of one particular case, the emitted harmonics are always circularly polarized. This provides for a convenient method to generate circular polarization in a frequency regime where this is not straightforward.

In the third section we display the results of numerical computations of the emission rates for representative situations. We cover the case of two incommensurate frequencies with perpendicular polarizations and discuss the emitted spectra in terms of the sidebands induced by one field on the harmonics of the other, the extent of the plateau, and the semiclassical model for various intensity ratios of the driving fields. For two incident circular polarizations co-rotating or counter-rotating in the same plane we compare the emitted spectra with each other and the previous case. For the experimentally important case where one incident field is the first harmonic of the other there are data to compare with [9,10]. We look at the various polarization configurations including the important case of parallel polarizations and provide examples of the strong dependence of the harmonics on the relative phase between the two fields. We also discuss the scaling of the harmonics when one driving field is weak compared to the other and investigate the harmonic spectrum for incident fields which are almost, but not exactly, perpendicular. Finally, we consider two incident perpendicular polarizations for a frequency ratio of 3:1 which allow, in principle, for the generation of harmonics with arbitrary elliptic including circular polarization. Conclusions are given in the end.

II. HIGH-HARMONIC EMISSION RATES

Our starting point is the expression [I, Eq. (3.7)] for the Fourier transform of the expectation value of the dipole moment of the quasienergy ground state which we repeat here for convenience:

$$\mathbf{d}(\Omega)=\frac{e}{m\kappa^2}\left[\frac{2\pi i}{m}\right]^{1/2}\times\int_{-\infty}^{\infty}dt\,e^{i\Omega t}\int_{-\infty}^{t}dt'dt''e^{-i(Et''-E^*t')}\times w(t')^*w(t'')(t'-t''-i\epsilon)^{-5/2}\times\mathcal{F}(t;t',t'')e^{-i\mathcal{M}(t',t'')}\,, \quad (2.1)$$

where

$$\mathcal{F}(t;t',t'')=e(t-t'')\int_{t'}^{t}d\tau\,\mathbf{A}(\tau)-e(t-t')\int_{t''}^{t}d\tau\,\mathbf{A}(\tau) \quad (2.2)$$

and

$$\mathcal{M}(t',t'')=\frac{e^2}{2m}\left[\int_{t''}^{t'}d\tau\,\mathbf{A}(\tau)^2-\frac{1}{t'-t''}\left[\int_{t''}^{t'}d\tau\,\mathbf{A}(\tau)\right]^2\right]. \quad (2.3)$$

The quantity E is the complex quasienergy of the ground state and $w(t)$ is defined via Eqs. (2.14) and (2.26) of I,

$$\lim_{r\to 0}\frac{\partial}{\partial r}r\Psi(\mathbf{r},t)\equiv e^{-iEt}w(t)\,, \quad (2.4)$$

with $\Psi(\mathbf{r},t)$ the quasienergy wave function of the ground state. We will replace $w(t)$ by a constant throughout this paper,

$$w(t)\to a_0=(2\pi)^{-1/2}(2m|E_0|)^{3/4}\,, \quad (2.5)$$

where a_0 is determined from the normalization of the ground state according to Eq. (2.40) of I. The validity of this approximation has been discussed in I.

We will evaluate the dipole moment (2.1) for a superposition of two monochromatic fields either both linearly polarized or both circularly polarized in the same plane with equal or opposite handedness.

A. Two linear polarizations

We consider a field with vector potential

$$\mathbf{A}(t)=a_1\epsilon_1\cos(\omega_1 t+\delta_1)+a_2\epsilon_2\cos(\omega_2 t+\delta_2)\,, \quad (2.6)$$

where ϵ_1 and ϵ_2 are arbitrary unit vectors. In this case

$$\mathcal{F}(t;t',t'')=\frac{ie}{2}\sum_{i=1}^{2}\frac{a_i}{\omega_i}\epsilon_i e^{i(\omega_i t+\delta_i)}\times[\tau'-\tau''+\tau''e^{-i\omega_i\tau'}-\tau'e^{-i\omega_i\tau''}]+\text{c.c.} \quad (2.7)$$

and

$$\mathcal{M}(t',t'')=-\sum_{i=1}^{2}\eta_i V_i(\tau)-\sum_{i=1}^{2}\cos[\omega_i(\tau'+\tau''-2t)-2\delta_i]z_i(\tau'-\tau'')-\cos\left[\frac{\omega_1+\omega_2}{2}(\tau'+\tau''-2t)-\delta_1-\delta_2\right]z_+(\tau'-\tau'')-\cos\left[\frac{\omega_1-\omega_2}{2}(\tau'+\tau''-2t)-\delta_1+\delta_2\right]z_-(\tau'-\tau'')\,, \quad (2.8)$$

where

$$\tau'=t-t',\quad \tau''=t-t'' , \tag{2.9}$$

$$\mathrm{sinc}x=\frac{\sin x}{x} , \tag{2.10}$$

$$V_i(\tau)=\omega_i\tau\left[1-\mathrm{sinc}^2\left[\frac{\omega_i\tau}{2}\right]\right] , \tag{2.11}$$

$$\eta_i=\frac{e^2a_i^2}{4m\omega_i} , \tag{2.12}$$

$$z_i(\tau)=\eta_i\omega_i\tau\left[\mathrm{sinc}(\omega_i\tau)-\mathrm{sinc}^2\left[\frac{\omega_i\tau}{2}\right]\right] , \tag{2.13}$$

$$z_{\pm}(\tau)=\boldsymbol{\epsilon}_1\cdot\boldsymbol{\epsilon}_2\frac{e^2a_1a_2}{2m}\tau\left[\mathrm{sinc}\left[\frac{\omega_1\pm\omega_2}{2}\tau\right]-\mathrm{sinc}\left[\frac{\omega_1}{2}\tau\right]\mathrm{sinc}\left[\frac{\omega_2}{2}\tau\right]\right] . \tag{2.14}$$

The generalization of these expressions to an arbitrary number of monochromatic fields is obvious.

The integration over t in the expression (2.1) for the dipole moment $\mathbf{d}(\Omega)$ can now be carried out if we expand the terms in $\exp(-i\mathcal{M})$ that depend on t in terms of Bessel functions. The result is

$$\begin{aligned}\mathbf{d}(\Omega)=&-\frac{e^2\pi}{2m\kappa^2}\left[\frac{2\pi i}{m}\right]^{1/2}|a_0|^2\\&\times\int_{-\infty}^{\infty}\frac{d\tau}{(\tau+i\epsilon)^{5/2}}\int_{|\tau|}^{\infty}d\sigma\, e^{i|E_0|\tau}\exp\left[i\sum_{i=1}^{2}\eta_iV_i(\tau)\right]\\&\times\sum_{n_1,n_2,n_+,n_-}i^{n_1+n_2+n_++n_-}e^{-i(\mu_1\delta_1+\mu_2\delta_2)}J_{n_1}[z_1(\tau)]J_{n_2}[z_2(\tau)]J_{n_+}[z_+(\tau)]J_{n_-}[z_-(\tau)]\\&\times\sum_{i=1}^{2}\epsilon_i\frac{a_i}{\omega_i}[e^{i\delta_i}\delta(\Omega-\mu_1\omega_1-\mu_2\omega_2+\omega_i)e^{(i\sigma/2)(\Omega+\omega_i)}f(\sigma,\tau,\omega_i)\\&-e^{-i\delta_i}\delta(\Omega-\mu_1\omega_1-\mu_2\omega_2-\omega_i)e^{(i\sigma/2)(\Omega-\omega_i)}f(\sigma,\tau,\omega_i)^*] ,\end{aligned} \tag{2.15}$$

where

$$\begin{aligned}\mu_1&=2n_1+n_++n_- ,\\ \mu_2&=2n_2+n_++n_- ,\end{aligned} \tag{2.16}$$

and

$$\begin{aligned}f(\sigma,\tau,\omega)=&\tau+\tfrac{1}{2}(\sigma-\tau)e^{-(i\omega/2)(\sigma+\tau)}\\&-\tfrac{1}{2}(\sigma+\tau)e^{-(i\omega/2)(\sigma-\tau)} .\end{aligned} \tag{2.17}$$

On the way from Eq. (2.1) to Eq. (2.15) we have transformed variables according to

$$\sigma=\tau'+\tau'',\quad \tau=\tau'-\tau'' \tag{2.18}$$

and replaced the quasienergy E by its field-free value $-|E_0|$.

The summations in Eq. (2.15) extend over all integer values of n_1,n_2,n_+, and n_-. Consequently, both $\mu_1+\mu_2$ and $\mu_1-\mu_2$ in Eq. (2.16) are even. Hence μ_1 and μ_2 must be either both even or both odd. Equation (2.15) then shows that the total number of photons absorbed from both fields must be odd. It also displays the appropriate powers of the phases $\exp(-i\delta_i)$ for each case.

The integrals over σ that remain to be done are

$$\int_{|\tau|}^{\infty}d\sigma\, f(\sigma,\tau,\omega)e^{i(\sigma/2)(\Omega+\omega)}=\frac{4i}{\Omega^2}e^{(i/2)\Omega|\tau|}g(\tau,\omega) , \tag{2.19}$$

where

$$g(\tau,\omega)=\sin\left[\frac{\omega\tau}{2}\right]-\frac{\omega\tau}{2(1+\omega/\Omega)}e^{(i/2)\omega|\tau|} \tag{2.20}$$

and

$$\int_{|\tau|}^{\infty}d\sigma\, f^*(\sigma,\tau,\omega)e^{i(\sigma/2)(\Omega-\omega)}=\frac{4i}{\Omega^2}e^{(i/2)\Omega|\tau|}g(\tau,-\omega) . \tag{2.21}$$

Each term in the sum (2.15) involves an odd number of photons from one field and an even number of photons from the other. It is useful to rearrange the sum such that the terms with $\Omega=(2m_1+1)\omega_1+2m_2\omega_2$ and $\Omega=2m_1\omega_1+(2m_2+1)\omega_2$ are displayed explicitly. Rearranging the summation as described and performing the above integrations we can write the dipole moment as

$$\mathbf{d}(\Omega)=-\frac{e^2}{\kappa^2\Omega^2}\left[\frac{2\pi i}{m}\right]^{3/2}|a_0|^2$$
$$\times\int_{-\infty}^{\infty}\frac{d\tau}{(\tau+i\epsilon)^{5/2}}e^{i|E_0|\tau}e^{(i/2)\Omega|\tau|}e^{i\sum\eta_i V_i(\tau)}$$
$$\times\sum_{m_1m_2n_1n_2}i^{2m_1+n_2-n_1}e^{-2i(m_1\delta_1+m_2\delta_2)}J_{m_1+m_2-n_1-n_2}(z_+)$$
$$\times\left\{\epsilon_1\frac{a_1}{\omega_1}J_{n_2}(z_2)[ig(\tau,\omega_1)J_{n_1+1}(z_1)-g(\tau,-\omega_1)J_{n_1}(z_1)]\right.$$
$$\times[e^{-i\delta_1}\delta(\Omega-(2m_1+1)\omega_1-2m_2\omega_2)J_{m_1-m_2-n_1+n_2}(z_-)$$
$$-ie^{-i\delta_2}\delta(\Omega-2m_1\omega_1-(2m_2+1)\omega_2)J_{m_1-m_2-n_1+n_2-1}(z_-)]$$
$$+i\epsilon_2\frac{a_2}{\omega_2}J_{n_1}(z_1)[ig(\tau,\omega_2)J_{n_2+1}(z_2)-g(\tau,-\omega_2)J_{n_2}(z_2)]$$
$$\times[e^{-i\delta_1}\delta(\Omega-(2m_1+1)\omega_1-2m_2\omega_2)J_{m_1-m_2-n_1+n_2+1}(z_-)$$
$$\left.-ie^{-i\delta_2}\delta(\Omega-2m_1\omega_1-(2m_2+1)\omega_2)J_{m_1-m_2-n_1+n_2}(z_-)]\right\}. \tag{2.22}$$

It can be checked that this expression is symmetric with respect to the interchange of the parameters of the two fields, i.e., $(\epsilon_1,a_1,\omega_1,\delta_1)\leftrightarrow(\epsilon_2,a_2,\omega_2,\delta_2)$. In the limit where one field is turned off, Eq. (2.22) agrees with Eq. (3.14) of I.

Lengthy as the expression (2.22) for the dipole moment is, it reveals several features of the spectrum of higher harmonics. As already mentioned, harmonic emission occurs at the frequencies $\Omega=(2m_1+1)\omega_1+2m_2\omega_2$ and $\Omega=2m_1\omega_1+(2m_2+1)\omega_2$, so that the total number of photons absorbed from the field is odd as required by parity conservation. If ω_1 and ω_2 are incommensurate, then all of these frequencies are different and the corresponding rates of emission are given by the squares of the coefficients of the respective δ functions in Eq. (2.22). These coefficients consist of twofold series of products of Bessel functions. In the incommensurate case, nothing observable will depend on the phases δ_1 and δ_2. If ω_1 and ω_2 are commensurate, then different values of m_1 and m_2 may yield the same emitted frequency Ω and all contributions to one particular Ω must be summed up before the square is taken. In this case the rate of emission will depend on some linear combination of the phases δ_1 and δ_2. We will discuss some commensurate cases in more detail below. The polarization of the emitted harmonics will, in general, be elliptic, since each δ function has one coefficient proportional to ϵ_1 and another one proportional to ϵ_2 and their ratio will, in general, be complex. More specific statements cannot be made without evaluating $\mathbf{d}(\Omega)$ explicitly. The expression (2.22) shows that each field generates even sidebands to the odd harmonics of the other.

For numerical purposes, it is convenient to rewrite the expression (2.22) for the dipole moment $\mathbf{d}(\Omega)$ such that the integration extends over positive values of τ only. The resulting form is

$$\mathbf{d}(\Omega)=-\frac{2e^2}{\kappa^2\Omega^2}\left[\frac{2\pi}{m}\right]^{3/2}|a_0|^2$$
$$\times\int_0^{\infty}\frac{d\tau}{\tau^{5/2}}e^{(i/2)\Omega\tau}\sum_{m_1m_2n_1n_2}(-1)^{m_1}e^{-2i(m_1\delta_1+m_2\delta_2)}J_{m_1+m_2-n_1-n_2}(z_+)$$
$$\times\left\{\epsilon_1\frac{a_1}{\omega_1}J_{n_2}(z_2)\right.$$
$$\times[J_{m_1-m_2-n_1+n_2}(z_-)e^{-i\delta_1}\delta(\Omega-(2m_1+1)\omega_1-2m_2\omega_2)G^{(+)}_{n_1;n_1,n_2}(\tau,\omega_1,z_1)$$
$$-J_{m_1-m_2-n_1+n_2-1}(z_-)e^{-i\delta_2}$$
$$\times\delta(\Omega-2m_1\omega_1-(2m_2+1)\omega_2)G^{(-)}_{n_1;n_1,n_2}(\tau,\omega_1,z_1)]$$
$$+\epsilon_2\frac{a_2}{\omega_2}J_{n_1}(z_1)$$
$$\times[J_{m_1-m_2-n_1+n_2+1}(z_-)e^{-i\delta_1}\delta(\Omega-(2m_1+1)\omega_1-2m_2\omega_2)$$
$$\times G^{(-)}_{n_2;n_1,n_2}(\tau,\omega_2,z_2)+J_{m_1-m_2-n_1+n_2}(z_-)e^{-i\delta_2}$$
$$\left.\times\delta(\Omega-2m_1\omega_1-(2m_2+1)\omega_2)G^{(+)}_{n_2;n_1,n_2}(\tau,\omega_2,z_2)]\right\}, \tag{2.23}$$

where

$$G^{(+)}_{n;n_1,n_2}(\tau,\omega,z)=J_{n+1}(z)g(\tau,\omega)\sin\alpha_{n_1n_2}(\tau)+J_n(z)g(\tau,-\omega)\cos\alpha_{n_1n_2}(\tau)\ , \tag{2.24}$$

$$G^{(-)}_{n;n_1,n_2}(\tau,\omega,z)=J_{n+1}(z)g(\tau,\omega)\cos\alpha_{n_1n_2}(\tau)-J_n(z)g(\tau,-\omega)\sin\alpha_{n_1n_2}(\tau)\ , \tag{2.25}$$

and

$$\alpha_{n_1n_2}(\tau)=|E_0|\tau+\sum_{i=1}^{2}\eta_i V_i(\tau)+\frac{\pi}{2}(n_2-n_1)-\frac{\pi}{4}\ . \tag{2.26}$$

A significant simplification occurs when the two linearly polarized fields are perpendicular so that $z_+=z_-=0$ [cf. Eq. (2.14)]. In this event the fourfold sum reduces to a twofold sum (where $n_1=m_1$ and $n_2=m_2$) and the terms proportional to $G^{(-)}$ do not contribute. Hence for $\epsilon_1\cdot\epsilon_2=0$,

$$\begin{aligned}\mathbf{d}(\Omega)=&-\frac{2e^2}{\kappa^2\Omega^2}\left[\frac{2\pi}{m}\right]^{3/2}|a_0|^2\\ &\times\int_0^\infty\frac{d\tau}{\tau^{5/2}}e^{(i/2)\Omega\tau}\sum_{m_1m_2}(-1)^{m_1}e^{-2i(m_1\delta_1+m_2\delta_2)}\\ &\times\left\{\epsilon_1\frac{a_1}{\omega_1}J_{m_2}(z_2)e^{-i\delta_1}\delta(\Omega-(2m_1+1)\omega_1-2m_2\omega_2)G^{(+)}_{m_1;m_1,m_2}(\tau,\omega_1,z_1)\right.\\ &+\epsilon_2\frac{a_2}{\omega_2}J_{m_1}(z_1)e^{-i\delta_2}\delta(\Omega-2m_1\omega_1-(2m_2+1)\omega_2)\\ &\left.\times G^{(+)}_{m_2;m_1,m_2}(\tau,\omega_2,z_2)\right\}\ .\end{aligned} \tag{2.27}$$

In this case and only in this case is the polarization of the emitted harmonic photon identical with the polarization of that incident field from which the odd number of photons was absorbed.

When ω_1 and ω_2 are commensurate the two δ functions in Eq. (2.27) may specify the same frequency Ω. This happens when $(2m_1+1)\omega_1+2m_2\omega_2=2m_1'\omega_1+(2m_2'+1)\omega_2$, that is, when

$$\frac{\omega_1}{\omega_2}=\frac{2(m_2'-m_2)+1}{2(m_1-m_1')+1} \tag{2.28}$$

is the ratio of two odd integers. The simplest case is $\omega_1/\omega_2=3$. If in such a case the ratio of the coefficients of the two δ functions in Eq. (2.27) (where $\epsilon_1\cdot\epsilon_2=0$) is equal to $\pm i$, the respective harmonic is emitted with circular polarization. Since for given frequencies three real quantities are at our disposal, viz. a_1,a_2, and the applicable combination of the phases δ_1 and δ_2 [such as given, for the case where $\omega_1=2\omega_2$, in Eq. (2.32) below], it appears likely that this is possible. Hence, there is a prospect of generating circular polarization in a frequency range where this is difficult to achieve by other means.

From the point of view of experimental feasibility the case where

$$\omega_1=2\omega_2\equiv 2\omega \tag{2.29}$$

is distinguished. In this case the dipole moment (2.23) reduces to

$$\begin{aligned}\mathbf{d}(\Omega)=&-\frac{2e^2}{\kappa\omega\Omega^2}\left[\frac{2\pi}{m}\right]^{3/2}|a_0|^2\\ &\times\int_0^\infty d\tau\,\tau^{-5/2}e^{(i/2)\Omega\tau}\\ &\times\sum_n e^{2in(\delta_2-\delta_1)}(-1)^n\\ &\times\sum_{n_1n_2}(-1)^{n_1+n_2}e^{2i(n_1+n_2)\delta}\\ &\times\{\delta(\Omega-2n\omega)e^{i\delta}[-\tfrac{1}{2}a_1\epsilon_1J_{n_2}(z_2)J_{N+2}(z_-,z_+,2\delta)G^{(+)}_{n_1;n_1n_2}(\tau,2\omega,z_1)\\ &+a_2\epsilon_2J_{n_1}(z_1)J_{N+1}(z_-,z_+,2\delta)G^{(-)}_{n_2;n_1n_2}(\tau,\omega,z_2)]\\ &+\delta(\Omega-(2n+1)\omega)e^{-i\delta_2}[\tfrac{1}{2}a_1\epsilon_1J_{n_2}(z_2)J_{N+1}(z_-,z_+,2\delta)G^{(-)}_{n_1;n_1n_2}(\tau,2\omega,z_1)\\ &+a_2\epsilon_2J_{n_1}(z_1)J_N(z_-,z_+,2\delta)G^{(+)}_{n_2;n_1n_2}(\tau,\omega,z_2)]\}\ ,\end{aligned} \tag{2.30}$$

where

$$N=2(2n_1+n_2-n)\ , \tag{2.31}$$

$$\delta=\delta_1-2\delta_2\ , \tag{2.32}$$

and we have defined the generalized Bessel function

$$J_n(u_1,u_2,\phi)=\sum_s J_{3s+n}(u_1)J_s(u_2)e^{is\phi}\ . \tag{2.33}$$

The dipole moment (2.30) displays even as well as odd harmonics of the frequency $\omega\equiv\omega_2$. The odd harmonics can be emitted without participation of field 1 (with $\omega_1=2\omega$). In the same way the even harmonics with odd n can be emitted without participation of field 2. For the emission of the even harmonics with even n, however, at least two photons of field 2 must have been emitted or absorbed. Thus we expect three series of harmonics (odd Ω/ω, even Ω/ω with odd n, even Ω/ω with even n) with distinctly different scaling behavior with respect to the intensities of the two fields. It is important to notice that the harmonic emission rates calculated from Eq. (2.30) depend on the phases δ_1 and δ_2 of the field (2.6) only through the combination δ in Eq. (2.32) (which is not equal to the phase difference $\delta_1-\delta_2$).

Again, the simplest case occurs when the two polarizations are perpendicular. Only the first and the last terms on the right-hand side (rhs) of Eq. (2.30) survive and yield

$$\begin{aligned}\mathbf{d}(\Omega)=&-\frac{2e^2}{\kappa\omega\Omega^2}\left[\frac{2\pi}{m}\right]^{3/2}|a_0|^2\\
&\times\int_0^\infty d\tau\,\tau^{-5/2}e^{(i/2)\Omega\tau}\\
&\times\sum_n e^{-2in\delta_2}\sum_{n_1}(-1)^{n_1}e^{-2in_1\delta}\\
&\times\{\delta(\Omega-2n\omega)e^{-i\delta}\tfrac{1}{2}a_1\boldsymbol{\epsilon}_1J_{n-1-2n_1}(z_2)G^{(+)}_{n_1;n_1,n-1-2n_1}(\tau,2\omega,z_1)\\
&+\delta(\Omega-(2n+1)\omega)e^{-i\delta_2}a_2\boldsymbol{\epsilon}_2J_{n_1}(z_1)G^{(+)}_{n-2n_1;n_1,n-2n_1}(\tau,\omega,z_2)\}\ .\end{aligned} \tag{2.34}$$

B. Two circular polarizations

We consider the case of two monochromatic fields with different frequencies rotating in the same plane, either in the same direction or opposite to each other, so that

$$\begin{aligned}\mathbf{A}(t)&=a_1(\boldsymbol{\epsilon}_1\cos\omega_1t+\boldsymbol{\epsilon}_2\sin\omega_1t)+a_2[\boldsymbol{\epsilon}_1\cos(\omega_2t+\delta)\pm\boldsymbol{\epsilon}_2\sin(\omega_2t+\delta)]\\
&=\frac{1}{\sqrt{2}}\{\mathbf{e}_+(a_1e^{-i\omega_1t}+a_2e^{\mp i(\omega_2t+\delta)})+\text{c.c.}\}\ ,\end{aligned} \tag{2.35}$$

where

$$\mathbf{e}_+=\frac{1}{\sqrt{2}}(\boldsymbol{\epsilon}_1+i\boldsymbol{\epsilon}_2),\quad \mathbf{e}_-=\mathbf{e}_+^*\ , \tag{2.36}$$

and

$$\mathbf{e}_+^2=\mathbf{e}_-^2=0,\quad \mathbf{e}_+\cdot\mathbf{e}_-=1\ . \tag{2.37}$$

In Eq. (2.35) and throughout this section the upper (lower) sign corresponds to the fields rotating in the same (opposite) direction. We will refer to these two cases as equal (opposite) polarizations.

We now have in terms of the variables (2.18)

$$\begin{aligned}\mathcal{F}(t;t',t'')=\frac{ie}{\sqrt{2}}\mathbf{e}_+&\left\{\frac{a_1}{\omega_1}e^{-i\omega_1t}\left[e^{i\omega_1(\sigma/2)}\left[\tau\cos\frac{\omega_1}{2}\tau-i\sigma\sin\frac{\omega_1}{2}\tau\right]-\tau\right]\right.\\
&\left.\pm\frac{a_2}{\omega_2}e^{\mp i(\omega_2t+\delta)}\left[e^{\pm i\omega_2(\sigma/2)}\left[\tau\cos\frac{\omega_2}{2}\tau\mp i\sigma\sin\frac{\omega_2}{2}\tau\right]-\tau\right]\right\}+\text{c.c.}\end{aligned} \tag{2.38}$$

and

$$\mathcal{M}(t',t'')=-\sum\eta_iV_i(\tau)-z(\tau)\cos\left[\Delta\left[t-\frac{\sigma}{2}\right]\mp\delta\right] \tag{2.39}$$

with

$$\eta_i=\frac{e^2a_i^2}{2m\omega_i}\ , \tag{2.40}$$

$$\Delta=\omega_1\mp\omega_2\ , \tag{2.41}$$

$$z(\tau)=\frac{e^2a_1a_2}{m}\tau\left[\mathrm{sinc}(\tfrac{1}{2}\Delta\tau)-\mathrm{sinc}\left[\frac{\omega_1}{2}\tau\right]\mathrm{sinc}\left[\frac{\omega_2}{2}\tau\right]\right]\ , \tag{2.42}$$

and $V_i(\tau)$ still defined by Eq. (2.11). In comparison to Eqs. (2.12)–(2.16) notice the factor-of-2 difference in the definitions of η_i and $z(\tau)$ and the fact that $z(\tau)$ is proportional to either $z_+(\tau)$ or $z_-(\tau)$.

The dipole moment can now be computed in complete analogy with the above case of two linear polarizations. The result is

$$\begin{aligned}\mathbf{d}(\Omega)=&\frac{4e^2}{\kappa^2\Omega^2}\left[\frac{i\pi}{m}\right]^{3/2}|a_0|^2\\&\times\int_{-\infty}^{\infty}\frac{d\tau}{(\tau+i\epsilon)^{5/2}}e^{i\tau|E_0|}e^{(i/2)\Omega|\tau|}e^{i\sum\eta_iV_i(\tau)}\\&\times\sum_n i^ne^{\pm in\delta}\left\{\mathbf{e}_+\delta(\Omega-n\Delta-\omega_1)\left[\frac{a_1}{\omega_1}g(\tau,-\omega_1)J_n(z(\tau))\pm i\frac{a_2}{\omega_2}g(\tau,\mp\omega_2)J_{n+1}(z(\tau))\right]\right.\\&\left.-\mathbf{e}_-\delta(\Omega-n\Delta+\omega_1)\left[\frac{a_1}{\omega_1}g(\tau,\omega_1)J_n(z(\tau))\pm i\frac{a_2}{\omega_2}g(\tau,\pm\omega_2)J_{n-1}(z(\tau))\right]\right\}.\end{aligned} \tag{2.43}$$

The function $g(\tau,\omega)$ was defined in Eq. (2.20). It is easily checked that when either field is turned off ($a_1=0$ or $a_2=0$) no harmonics are emitted, as it should be. One may also check that for $\omega_1=\omega_2$ and opposite polarizations, the dipole moment (2.43) agrees with the result obtained in I, Eq. (3.14) for one field with appropriate elliptic polarization.

Comparing the dipole moments (2.22) and (2.43), the most pronounced difference is that for two linear polarizations a two-parameter set of harmonics is emitted while for two coplanar circular polarizations it is a one-parameter set with the harmonics spaced by $\Delta=\omega_1\mp\omega_2$. The fact that for equal polarizations the spacing is given by the frequency difference while for opposite polarizations it is given by the sum is physically appealing since in the first case the fields are corotating while they are counter-rotating in the second. A more rigorous explanation uses conservation of angular momentum. Consider the component J_z perpendicular to the plane of polarization and the case of equal polarizations. The ground state of our model atom has $J_z=0$. For each photon absorbed from either field, J_z changes by one unit in the same direction, say $\Delta J_z=+1$. For each photon emitted into either field, J_z is then diminished by one unit, $\Delta J_z=-1$. The emitted harmonic photon carries away one unit of J_z, $\Delta J_z=\pm1$. In order that the atom be left in its ground state after emission of the harmonic photon, it must have absorbed the same number n of photons from the high-frequency field that it emitted into the low-frequency field, plus one additional emission or absorption from either field, i.e., the allowed frequencies are $\Omega=n(\omega_1-\omega_2)\pm\omega_1$ or $\Omega=n(\omega_1-\omega_2)\pm\omega_2=(n\mp1)(\omega_1-\omega_2)\pm\omega_1$ as predicted by Eq. (2.43). For opposite polarizations, the analogous argument yields the spacing of $\Delta=\omega_1+\omega_2$.

For incommensurate frequencies, the δ functions in Eq. (2.43) define different frequencies Ω so that no emission rate will depend on the phase δ. If ω_1 and ω_2 are commensurate the situation is different. For opposite polarizations, closer inspection reveals that the two terms in Eq. (2.43) still define different frequencies. In all of these cases the polarization of the emitted harmonics is circular. For equal polarizations, however, the two series overlap provided that

$$\frac{\omega_1}{\omega_2}=\frac{k}{k-2} \tag{2.44}$$

for some integer k. If this is the case the emitted harmonics are no longer circularly polarized but have, in general, elliptic polarization depending on the phase δ. Their intensities, on the other hand, are still independent of this phase. An example, for the case where $\omega_1=2\omega_2$ so that $k=4$, will be considered explicitly below.

Again, it is convenient for numerical evaluation to convert the integration over τ to positive values. The dipole moment then assumes the form

$$\mathbf{d}(\Omega)=\frac{e^2}{\kappa^2\Omega^2}\left[\frac{4\pi}{m}\right]^{3/2}|a_0|^2 \times\int_0^\infty\frac{d\tau}{\tau^{5/2}}e^{(i/2)\Omega\tau} \times\sum_{n=-\infty}^{\infty}e^{\pm in\delta}\left\{\mathbf{e}_+\delta(\Omega-n\Delta-\omega_1)\left[\frac{a_1}{\omega_1}g(\tau,-\omega_1)J_n(z(\tau))\cos\alpha_n(\tau)\mp\frac{a_2}{\omega_2}g(\tau,\mp\omega_2)J_{n+1}(z(\tau))\sin\alpha_n(\tau)\right]\right.$$
$$\left.-\mathbf{e}_-\delta(\Omega-n\Delta+\omega_1)\left[\frac{a_1}{\omega_1}g(\tau,\omega_1)J_n(z(\tau))\cos\alpha_n(\tau)\mp\frac{a_2}{\omega_2}g(\tau,\pm\omega_2)J_{n-1}(z(\tau))\sin\alpha_n(\tau)\right]\right\} \tag{2.45}$$

with

$$\alpha_n(\tau)=|E_0|\tau+\sum_{i=1}^{2}\eta_i V_i(\tau)+\frac{\pi}{2}n-\frac{\pi}{4}\ . \tag{2.46}$$

The (commensurate) case where $\omega_1=2\omega_2\equiv2\omega$ illuminates the characteristic differences between equal and opposite polarizations. For equal polarizations $\Delta=\omega$ and the two δ functions in Eq. (2.45) generate the same series of frequencies. The dipole moment reduces to

$$\mathbf{d}(\Omega)=-\frac{e^2}{\kappa^2\Omega^2\omega}\left[\frac{4\pi}{m}\right]^{3/2}|a_0|^2 \times\int_0^\infty\frac{d\tau}{\tau^{5/2}}e^{(i/2)\Omega\tau}\sum e^{in\delta}\delta(\Omega-n\omega) \times\left\{e^{-2i\delta}\mathbf{e}_+\left[\frac{a_1}{2}g(\tau,-2\omega)J_{n-2}(z(\tau))\cos\alpha_n(\tau)-a_2g(\tau,-\omega)J_{n-1}(z(\tau))\sin\alpha_n(\tau)\right]\right.$$
$$\left.-e^{2i\delta}\mathbf{e}_-\left[\frac{a_1}{2}g(\tau,2\omega)J_{n+2}(z(\tau))\cos\alpha_n(\tau)-a_2g(\tau,\omega)J_{n+1}(z(\tau))\sin\alpha_n(\tau)\right]\right\} \tag{2.47}$$

with

$$z(\tau)=\frac{e^2a_1a_2}{m}\tau\,\mathrm{sinc}\left[\frac{\omega}{2}\tau\right][1-\mathrm{sinc}(\omega\tau)]\ . \tag{2.48}$$

Even as well as odd multiples of $\omega_2\equiv\omega$ are permitted with comparable intensities. The polarization of the emitted harmonics will in general be elliptic and dependent on the phase δ. The intensities, however, are independent of the phase. This becomes clear if one notices that the exponentials $\exp(\pm2i\delta)$ can be absorbed in the definition of the polarization vectors.

On the other hand, for opposite polarizations, $\Delta=3\omega$, and the two δ functions generate different series. The emitted frequencies are $\Omega=(3n\pm1)\omega$ (i.e., the frequencies $\Omega=3\omega,6\omega,\ldots,3n\omega$ are forbidden) and the polarization is always circular. The rates are clearly independent of the phase δ. The dipole moment is

$$\mathbf{d}(\Omega)=\frac{e^2}{\kappa^2\Omega^2\omega}\left[\frac{4\pi}{m}\right]^{3/2}|a_0|^2 \times\int_0^\infty\frac{d\tau}{\tau^{5/2}}e^{(i/2)\Omega\tau}\sum e^{in\delta}\left\{e^{i\delta}\mathbf{e}_+\delta(\Omega-(3n-1)\omega)\right.$$
$$\times\left[\frac{a_1}{2}g(\tau,-2\omega)J_{n-1}(z(\tau))\sin\alpha_n(\tau)-a_2g(\tau,\omega)J_n(z(\tau))\cos\alpha_n(\tau)\right]$$
$$+e^{-i\delta}\mathbf{e}_-\delta(\Omega-(3n+1)\omega)$$
$$\left.\times\left[\frac{a_1}{2}g(\tau,2\omega)J_{n+1}(z(\tau))\sin\alpha_n(\tau)-a_2g(\tau,-\omega)J_n(z(\tau))\cos\alpha_n(\tau)\right]\right\} \tag{2.49}$$

with

$$z(\tau)=\frac{e^2a_1a_2}{m}\tau\,\mathrm{sinc}\left[\frac{\omega}{2}\tau\right]\left[1-\mathrm{sinc}(\omega\tau)-\frac{4}{3}\sin^2\frac{\omega\tau}{2}\right]. \tag{2.50}$$

III. RESULTS

In what follows we will present the results of numerical evaluations of the expressions derived in the preceding section. In place of just one integral of the type (3.15) of I which determined the emission rate in the one-color case we now have, in general, to deal with two-dimensional sums of these integrals such as written down in Eqs. (2.23) and (2.30). Simultaneously, the size of the parameter space has increased tremendously owing to the addition of the second field. In the one-color case the spectrum depends on two dimensionless parameters, the scaled binding energy $|E_0|/\omega$, and field strength $\eta=U_p/\omega$. In addition, we now have one more scaled intensity, the frequency ratio, the relative phase (in case the frequencies are commensurate), and the polarization of the second field. Short of any systematic exploration of this parameter space, we will present here selected numerical results that shed some light on the rich and colorful properties of the two-color harmonics.

In all of the plots of this section the quantity $L(\Omega)$ defined by

$$d(\Omega)=2e\left[\frac{\pi}{m\omega}\right]^{1/2}\sum_k\delta[\Omega-(2k+1)\omega]L^*(\Omega) \tag{3.1}$$

will be represented.

A. Incommensurate frequencies and perpendicular polarizations

All of the following graphs provide illustrations of Eq. (2.27). When the two frequencies ω_1 and ω_2 are incommensurate, any frequency Ω can be arbitrarily closely approximated by $(2m_1+1)\omega_1+2m_2\omega_2$ or $2m_1\omega_1+(2m_2+1)\omega_2$ with suitable m_1 and m_2, that is, the spectrum of the emitted harmonics is, in principle, a quasicontinuum. This is a purely academic statement since most of these frequencies will be emitted with very low intensities. Figure 1 depicts a typical spectrum. Here $|E_0|/\omega_1=10$, $\omega_2=\sqrt{2}\omega_1$, $\eta_1=2$, and $\eta_2=1/10\sqrt{2}$ so that $U_{p2}=\omega_2\eta_2=0.1\omega_1$. The intensity ratio of the two fields is $I_2/I_1=0.1$. This figure displays those frequencies that are emitted with polarization ϵ_1, corresponding to the first term on the rhs of Eq. (2.27). One recognizes the odd harmonics of $\omega_1(1\le m_1\le 15)$ along with their sidebands ($-5\le m_2\le 5$, provided they are within the range of the graph). Many more frequencies are predicted by Eq. (2.27) corresponding to values of $m_1\le 1$ and large m_2 which are not included in Fig. 1 since their intensities are very low. The open squares give the intensities of the odd harmonics of ω_1 in the absence of the second field. A most noticeable effect of the second field is that the intensities of those harmonics $\Omega=(2m_1+1)\omega_1$ that are part of the plateau are diminished by about one order of magnitude. We have found this to be a very common effect. Only in few cases have we observed that the intensities of the odd harmonics were brightened by the addition of the second field, and then only by insubstantial amounts. Figure 1 allows for the identification both of the sidebands (m_1 fixed) of the odd harmonics of the first field as well as the series (m_2 fixed) where the second field contributes a definite number of photons. These latter curves exhibit (for not too large values of $|m_2|$) plateaus much like the one-color plateaus in the presence of just the first field. In particular, the $m_2=0$ series largely agrees with the one-color results except for the harmonics within the plateau which are dimmed by the second field as mentioned above. This effect may not come as a surprise: in a classical picture [4,5] that has been shown to incorporate a good deal of physical reality, harmonics are emitted when the electron returns to the center of the ion and drops back into the ground state. For incommensurate frequencies and perpendicular polarizations, a second field just impedes this process. The argument does not explain, however, why the harmonics outside the plateau

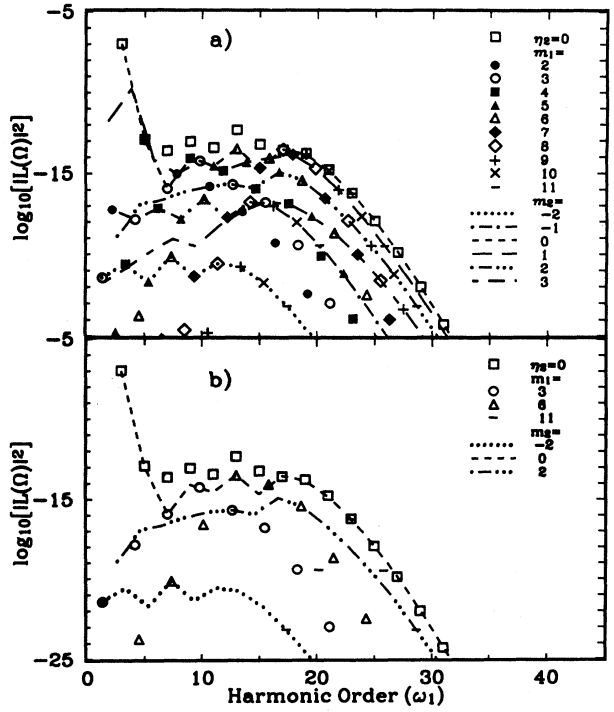

FIG. 1. $\log_{10}(|L(\Omega)|^2)$ vs harmonic order for $\omega_2=\sqrt{2}\omega_1$, $|E_0|=10\omega_1$, $\eta_1=2$, $\eta_2=(1/10)\sqrt{2}$. The open squares are the one-color, $\eta_2=0$, harmonic spectrum. (a) The other symbols are for the two-color case, each symbol is for a constant m_1 with $-5\le m_2\le 5$. The lines connect harmonics of constant m_2; (b) In order to facilitate orientation in (a) only a subset of the symbols is given here, viz., $m_1=3,6,11$ and the lines $m_2=-2,0,2$.

are unaffected by the second field. The sidebands of some harmonic with fixed m_1 (i.e., the set of harmonics with $m_1=$const, all m_2) are, for $m_1\omega_1$ beyond the plateau, almost symmetric with respect to $m_2\rightarrow -m_2$. If $m_1\omega_1$ lies within the one-color plateau there is some tendency of the second field to contribute a few photons, that is, the sidebands drop much faster for negative m_2 than for positive m_2.

Figure 2 shows the same situation, but with the intensity of the second field increased by a factor of 10, so that $\eta_2=1/\sqrt{2}$, $I_2=I_1$. In comparison, the most obvious feature of Fig. 2 is that now many frequencies are radiated with intensities stronger than in the one-color case. However, this is not so for $\Omega=(2m_1+1)\omega_1$: the odd harmonics of the first field are still suppressed by the addition of the second field. Otherwise, for example, next to $\Omega=17\omega_1(m_1=8,\ m_2=0)$ there is emission at $\Omega=16.66\omega_1(m_1=5,\ m_2=2)$ and $\Omega=17.48\omega_1(m_1=4,\ m_2=3)$ with intensities higher by almost two orders of magnitude. We notice that now within the plateau the second field has a very pronounced tendency to donate photons. This is most visibly expressed by the fact that in Fig. 2 the series with positive m_2 are much more intense than the one with $m_2=0$, and the sidebands to fixed m_1 are no longer symmetric with respect to $m_2\rightarrow m_2$. In general, the addition of a second field with $I_2=I_1$ and $\omega_2=\sqrt{2}\omega_1$ has multiplied the number of emitted frequencies and the most intense ones exceed the one-color harmonics by one to two orders of magnitude. The extent of the plateau, however, has hardly changed at all as compared to the one-color case. Moreover, doubling the intensity of the first field rather than adding the second generates more intense harmonics and at the same time extends the plateau.

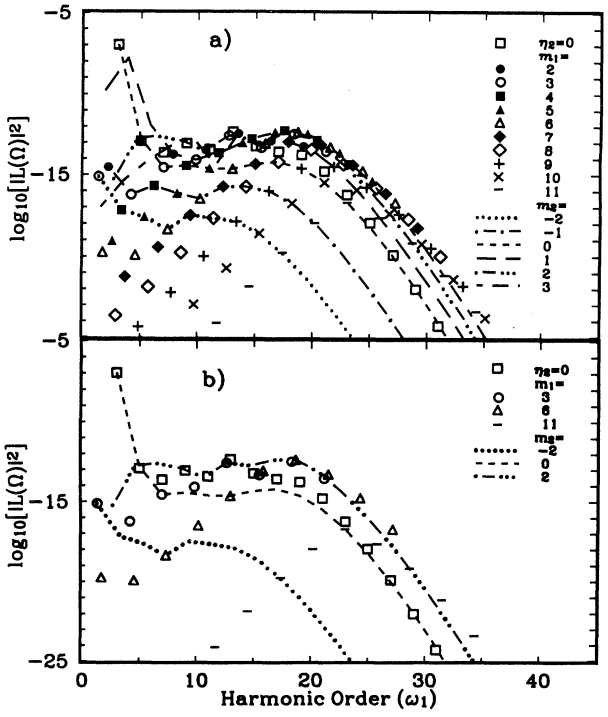

FIG. 2. $\log_{10}(|L(\Omega)|^2)$ vs harmonic order for $\omega_2=\sqrt{2}\omega_1$, $|E_0|=10\omega_1$, $\eta_1=2$, $\eta_2=1/\sqrt{2}$. The open squares are the one-color, $\eta_2=0$, harmonic spectrum. (a) The other symbols are for the two-color case, each symbol is for a constant m_1 with $-5\le m_2\le 5$. The lines connect harmonics of constant m_2; (b) In order to facilitate orientation in (a) only a subset of the symbols is given here, viz., $m_1=3,6,11$ and the lines $m_2=-2,0,2$.

B. Incommensurate frequencies and two coplanar circular polarizations

One single circularly polarized driving field generates no harmonics in dipole emission. This is no longer so if the driving field consists of two circularly polarized fields. In the preceding section we considered the case of two such fields such that the electric field vector of both fields rotates in the same plane. In what follows we will present explicit results for this situation, on the basis of Eq. (2.43).

Figure 3 shows the harmonic spectrum for the case where $\omega_2=(\omega_1/10)\sqrt{2}$ case. This case might represent an experiment where the low frequency field is from a CO_2 laser and the high frequency field is produced by a deep red, or near IR laser. Alternatively, the CO_2 laser could be the high-frequency source and the low-frequency field a microwave background. The binding energy is $|E_0|=5\omega_1$ and the intensities are such that $\eta_1=\eta_2=2$. Both the equal and opposite polarization cases are shown. The harmonics show the same plateau structure that is seen in the one-color case. In each case harmonics beyond the plateau that have the same polarization as the high-frequency field are more intense than those having the opposite polarization. Also in the falloff region the harmonics from fields of opposite polarization are more intense than those from fields with equal polarization. Harmonics in the plateau region occasionally violate these rules but in most cases they still hold.

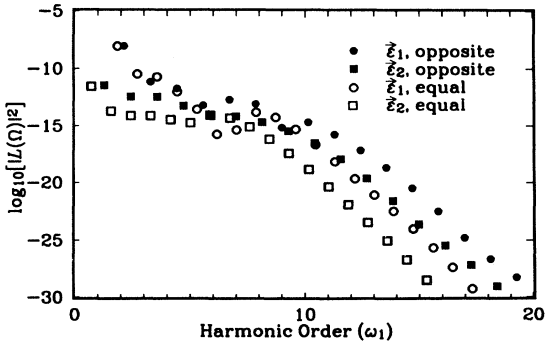

FIG. 3. $\log_{10}(|L(\Omega)|^2)$ vs harmonic order for the two-color circular case; $\omega_2=(\omega_1/10)\sqrt{2}$, $|E_0|=5\omega_1$, $\eta_1=\eta_2=2$. Field 1 is right circularly polarized. The open (solid) symbols are the harmonics produced when field 2 is right (left) circularly polarized. The polarization of the harmonics is right circular (circles) or left circular (squares) depending on the order.

These rules can be deduced from Eq. (2.43). This equation tells that for fixed n two frequencies are emitted, $\Omega=n\Delta+\omega_1$, with the polarization of the incident high-frequency field (ϵ_+), and $\Omega=n\Delta-\omega_1$ with the opposite polarization (ϵ_-). The two spectral lines of such a pair are separated in frequency by $2\omega_1$ and have roughly the same intensity. Within the plateau, the intensities do not depend on n in a regular fashion. Beyond the plateau, the intensities decrease by about one order of magnitude when n increases by 1. Hence, in this region Fig. 3 displays these pairs neatly separated, extending from the approximate center of the figure down to the lower right. For given frequency, the lines with the polarization of the incident high-frequency field (ϵ_+) are brighter than those with the opposite one (ϵ_-). Since Δ is larger for opposite than for equal polarizations, beyond the plateau a given frequency is more intense for driving fields with opposite polarizations. Notice that all harmonics are circularly polarized. This provides for a comparatively straightforward way of generating circular polarization at high frequency.

C. Commensurate frequencies ($\omega_2=2\omega_1$)

The two-color commensurate case nearest at hand is the case with the frequency of one field twice that of the other. Experimentally this is the most accessible case, and the one where most data are available at this time. The driving fields can be generated by doubling part of the output of a laser and then combining the doubled beam and the fundamental.

Eichmann *et al.* [10] published results of an experiment with frequencies $\omega_2=2\omega_1$. The intensities of the two fields were comparable. They measured the harmonic spectra in argon for the polarization conditions investigated in this paper, i.e., for two linearly polarized driving fields which were either perpendicular or parallel, for two circularly polarized fields corotating or counterrotating in the same plane, as well as the one-color spectra of each individual field. The experimental results were compared to the results of the δ-function potential theory. We have argued [22] that it is reasonable to adjust the binding energy of the model atom to the difference between the ground state and the first excited state of the real atom. Hence, for these calculations we will use 11.6 eV in place of the atomic binding energy of argon (15.6 eV). Figure 4 shows the harmonic spectra for this binding energy with intensities slightly less than those in the experiment. Figure 4(a) is a plot of the one-color spectra from the fields taken separately. Figure 4(b) shows the spectra for linearly polarized fields with perpendicular and parallel polarizations. Figure 4(c) shows the spectra when the two fields are circularly polarized. The spectra from both co- and counter-rotating driving fields are shown. Here we use parameters that are slightly different from the experiment. A direct comparison between the experimental data and the results of the δ-function potential has been carried out in Ref. [10]. The agreement was generally quite good except for the case of the co-rotating circular polarizations where the theoretical results were several orders of magnitude below the data. This could be at least partially explained by taking into account that in the experiment the circular polarization was not perfect.

In Fig. 4(a) the familiar features of one-color harmonics will be noticed. The fundamental pump field generates odd harmonics of ω_1, $\Omega=(2m+1)\omega_1$. The second harmonic field generates odd harmonics of the $2\omega_1$ field, $\Omega=(2m+1)2\omega_1$. The one-color spectrum from the fundamental alone has a plateau but, since η_2 is relatively small, the one-color spectrum produced by the second harmonic field does not have a plateau. When both fields are present there are both odd and even harmonics of ω_1. The intensities of the lower harmonics in Fig. 4(b) are enhanced over those in the same region in Fig. 4(a). This is possible since there is a great increase in the number of nonlinear processes that can generate a given harmonic. The harmonics generated by the parallel fields are, in general, stronger than those from perpendicular fields. The plateau is also longer in the parallel case. Several explanations can be put forward. First, there are a greater

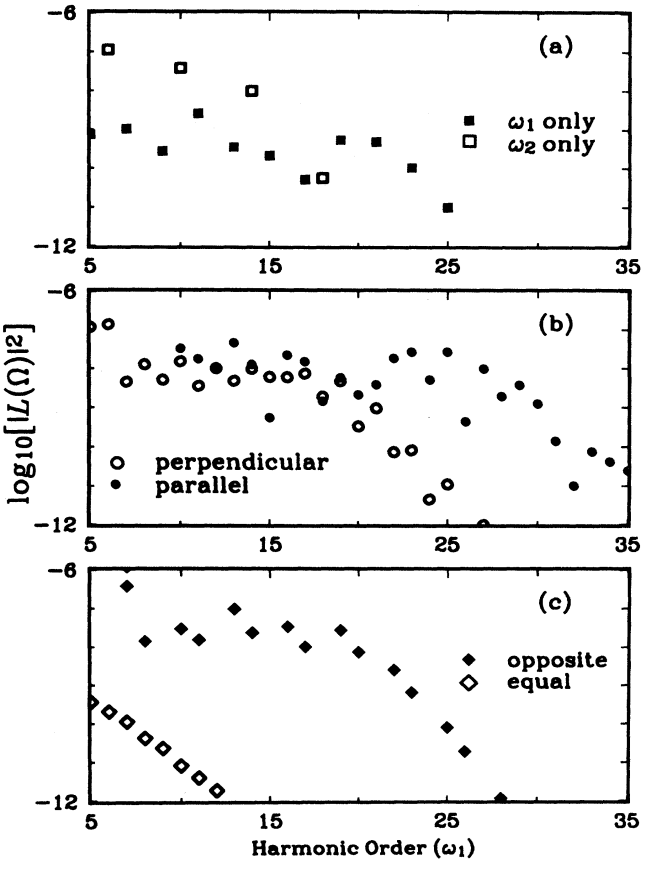

FIG. 4. $\log_{10}(|L(\Omega)|^2)$ vs harmonic order for $\omega_2=2\omega_1$, $|E_0|=7.24\omega_1$, $\eta_1=4$, $\eta_2=0.5$. (a) The one-color harmonic spectrum for field 1 only (solid squares), field 2 only (open squares). (b) Two linear fields with parallel field vectors (solid circles) and perpendicular field vectors (open circles). (c) Two circularly polarized fields with counter-rotating (solid diamonds) and corotating (open diamonds).

number of possible nonlinear processes (pathways) when the fields are parallel [compare Eqs. (2.23) and (2.27)]. The detailed argument can be found in Ref. [10]. Second, the classical theory discussed in the introduction suggests that for nonparallel polarizations the electron almost never returns to the center of the ion. With this model no harmonics can be produced in the nonparallel cases without introducing arguments based on the wave nature of the electron, or allowing the electrons to be released in the continuum with nonzero initial velocities.

Figure 4(c) shows the harmonics generated by two circularly polarized co- or counter-rotating fields. With two circularly polarized fields the number of photons absorbed from either field must differ by 1 in order to conserve angular momentum. For counter-rotating fields a given harmonic frequency can be generated by the process $m(2\omega_1)+(m\pm1)\omega_1=(3m\pm1)\omega_1$. Therefore the frequencies $3m\omega_1$ are not allowed. Since to lowest order in the driving fields only one pathway exists for each harmonic the harmonics are circularly polarized in the direction of the field which contributes the larger number of photons. (To higher order, there are more pathways which, however, only differ by additional pairs of emission and absorption of photons from one or the other field which does not affect the polarization.) Using the same angular momentum arguments when the driving fields are corotating the mixing processes are $(m\pm1)2\omega_1-(m\pm2)\omega_1=m\omega_1$. All integer harmonics of the low-frequency field are possible. For co-rotating fields processes of higher order are required to generate the same frequency (recall $\Delta=\omega_1-\omega_2$). Therefore, for similar frequencies the intensities of the harmonics generated by co-rotating fields are lower than those from counter-rotating fields. In the co-rotating case there are (again to lowest order in the driving fields) two pathways to each harmonic and the polarization of the harmonics is different from that of either incident field.

Figure 5 exhibits a typical example of the phase dependence of the harmonics for the case where the driving fields are linearly polarized and perpendicular to each other and $\delta_1=0$ so that $\delta=-2\delta_2$ [cf. Eq. (2.32)]. Equation (2.34) shows that the phase dependence of the intensities is caused by the existence of several pathways (numbered by the summation index n_1) which all contribute to the same harmonic. Each pathway involves a different number of emissions and absorptions of photons from either driving field. Hence each term enters the coherent sum (2.34), which makes up the dipole moment, with a different phase which latter is a function of the phases δ_1 and δ_2 of the driving fields. In short, the different pathways interfere constructively or destructively, depending on the phases of the driving fields. The effects are substantial: as a function of the phase δ_2 the ratios of the harmonics displayed in Fig. 5 differ by up to two orders of magnitude. This provides an impressive example of the possibilities of coherent control of the emission of high harmonics through the use of two driving fields.

One can see from Fig. 5 that the intensities are invariant against $\delta_2\rightarrow\delta_2+\pi$. Formally, this is easily inferred from Eq. (2.34). The underlying reason can be traced to the vector potential (2.6) where $\delta_2\rightarrow\delta_2+\pi$ corresponds (for perpendicular polarizations) to reversal of the 2 direction. Obviously, this has no effect on the emitted intensities. Notice that there is no symmetry with respect to $\delta_2\rightarrow-\delta_2$ which (for $\delta_1=0$) would be compensated by time reversal ($t\rightarrow-t$). It is clear that the harmonic spectra due to two fields that are related through time reversal will, in general, be different. In the context of the semiclassical model already mentioned repeatedly where the harmonics are due to recombination of the electron returning to the ion, time reversal interchanges the temporal order of the time where the electron is released in the continuum and the time where it returns. For two-color fields such as the field (2.6), the energies of the returning electrons are different in these two situations.

In Fig. 4(b) the plateau in the perpendicular harmonics ends before the one for the parallel harmonics. Figure 6 shows how the intensities of the harmonics in this region change as the angle between the two fields changes from perpendicular to parallel. The expression for the har-

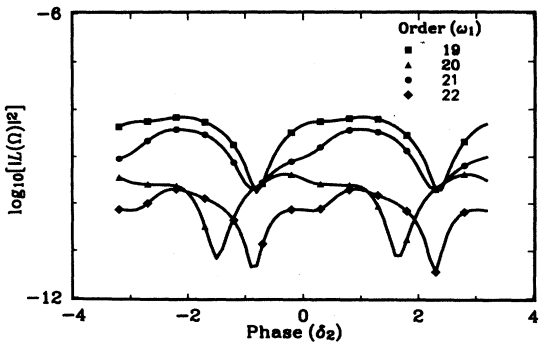

FIG. 5. $\log_{10}(|L(\Omega)|^2)$ vs the relative phase of two perpendicular linearly polarized fields $\omega_2=2\omega_1$, $\eta_1=4.0$, $\eta_2=0.5$, $|E_0|=7.24\omega_1$, $\delta_1=0$.

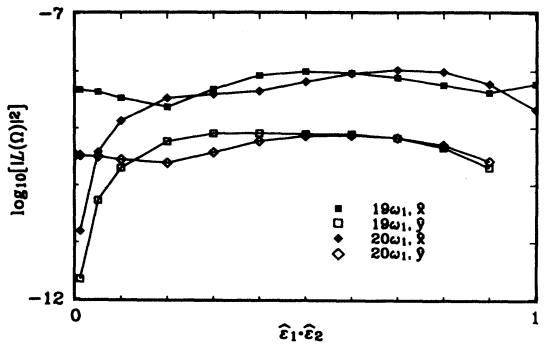

FIG. 6. $\log_{10}(|L(\Omega)|^2)$ vs the angle between the polarization vectors of the two fields, $\omega_2=2\omega_1$, $|E_0|=7.24\omega_1$, $\eta_1=4$, $\eta_2=0.5$, $\delta_1=\delta_2=0$. The solid symbols represent the portion of the harmonic polarized in the direction of the first field. The open symbols are the portion of the harmonic polarized in the perpendicular direction.

monic, Eq. (2.23), has two terms: one polarized in the ϵ_1 direction and the other in the ϵ_2 direction. The plot shows the projections of the dipole moment on the $\hat{x}$ direction, defined to be in the direction ϵ_1, and the $\hat{y}$ direction which is perpendicular to $\hat{x}$. When the fields are perpendicular $\epsilon_2=\hat{y}$. In this case the odd harmonics are completely polarized in the $\hat{x}$ direction and the even harmonics are completely polarized in the $\hat{y}$ direction. When the fields are parallel, $\epsilon_1=\epsilon_2=\hat{x}$, and the harmonics are completely polarized in this direction. The $\hat{y}$ components of the odd harmonics and the $\hat{x}$ components of the even harmonics turn on rapidly as the second field is turned from perpendicular. By the time $\epsilon_1\cdot\epsilon_2\approx 0.1$ the $\hat{y}$ component of the odd harmonic has risen to the same magnitude as the $\hat{y}$ component of the even harmonic. The magnitude of the perpendicular components is also nearly equal. From this point on the intensities of the components do not change by more than an order of magnitude until the $\hat{y}$ components vanish when the fields become parallel. The experimental consequences for harmonics generated by perpendicularly polarized driving fields will be discussed below.

The harmonics of parallel and perpendicular fields have distinct characteristics. When the driving fields are perpendicular, the even harmonics are polarized in the same direction as the first field, the odd harmonics are polarized in the same direction as the second field, and at and beyond the edge of the plateau the harmonics polarized in the direction of the weaker field are less intense than the others. In the parallel case all harmonics are polarized in the same direction as the two driving fields and the intensities of the even and odd harmonics in the falloff region do not alternate. As the angle between the fields changes the characteristics of the harmonics change from one type to the other. The change is more abrupt than gradual. The harmonics have the characteristics of perpendicular fields when the $\hat{x}$ ($\hat{y}$) components of the even (odd) harmonics are much less than the $\hat{x}$ ($\hat{y}$) components of the odd (even) harmonics. This condition is met when the maximum value of $|z_{\pm}(\tau)|\ll 1$, which means $\epsilon_1\cdot\epsilon_2\sqrt{\eta_1\eta_2}\ll 1$. Otherwise, the characteristics of the harmonics are more like those of harmonics from parallel driving fields. The harmonics of driving fields that are neither perpendicular nor parallel have one characteristic that sets them apart from either of the extremes: their polarization can have components in both the $\hat{x}$ and $\hat{y}$ directions. That is, they can potentially have any polarization. In order to investigate these effects experimentally the relative polarization of the two fields must be controlled with a high degree of accuracy.

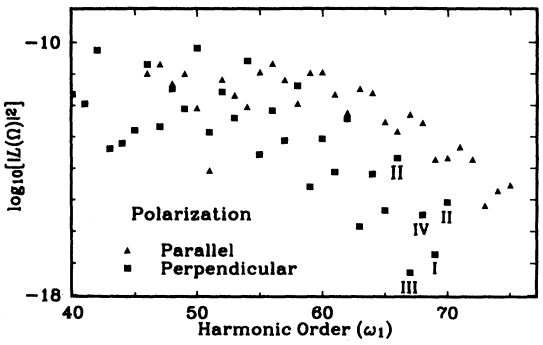

FIG. 7. $\log_{10}|L(\Omega)|^2$ vs harmonic order, $\omega_2=2\omega_1$, $|E_0|=16.82\omega_1$, $\eta_2=5.0$, $\eta_1=0.5$, $\delta_1=\delta_2=0$. Both the parallel and perpendicular driving field cases are shown.

Perry and Crane have performed experiments with the high-frequency field stronger than the low-frequency field [9]. This change in relative intensities from the situation of Ref. [10] dramatically alters the characteristic features of the harmonic spectrum. Figure 7 shows the spectrum calculated using the δ-function potential model for the experimental parameters of Ref. [9]. As in the previous case the plateau for harmonics of the perpendicular driving fields ends before that for parallel driving fields. In the falloff region a clear pattern can be seen in the perpendicular harmonics. The odd harmonics are much less intense than the even harmonics. Also, the brightness of even harmonics alternates in a regular fashion as does the brightness of the odd harmonics. There is some variation in the brightness of the parallel harmonics, too, but with a smaller amplitude. The calculated spectrum of Fig. 7 is in qualitative disagreement with the experimental results of Perry and Crane [9], notably for perpendicular driving fields [cf. Fig. 2(b) of Ref. [9]]. Below we will pinpoint a possible reason of this discrepancy.

These patterns in the intensity of the perpendicular harmonics are a result of the behavior of only a few processes which dominate at these intensities. When one of the fields is much smaller than the other the dominant processes are the ones with the lowest number of weak field photons. The scaling behavior of the various harmonics when $\eta_1\ll 1$ is given in Table I. It can be ex-

TABLE I. Frequencies and scaling laws for the lowest order channels when $\omega_2=2\omega_1$, $\eta_1\ll\eta_2\ll 1$.

Type	Frequency	ω_1 photons	ω_2 photons	Power law
I	$\Omega=(4m+1)\omega_1$	1	$2m$	$\eta_2^{2m}\eta_1$
II	$\Omega=2(2m+1)\omega_1$	0	$2m+1$	η_2^{2m+1}
III	$\Omega=(4m-1)\omega_1$	-1	$2m$	$\eta_2^{2m}\eta_1$
IV	$\Omega=(4m)\omega_1$	2	$2m-1$	$\eta_2^{2m-1}\eta_1^2$
		-2	$2m+1$	$\eta_2^{2m+1}\eta_1^2$

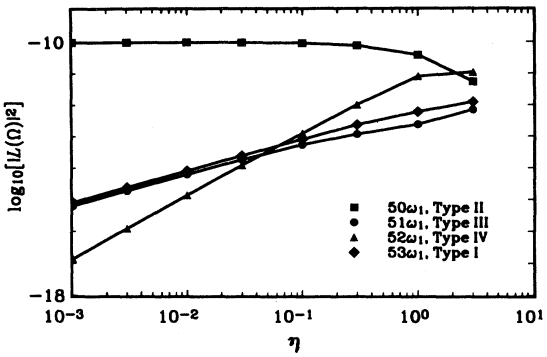

FIG. 8. The dependence of the harmonics from two perpendicular fields on η_1 when $\eta_1 \ll 1$, $\eta_2 = 5.0$, $\omega_2 = 2\omega_1$, $|E_0| = 16.82\omega_1$.

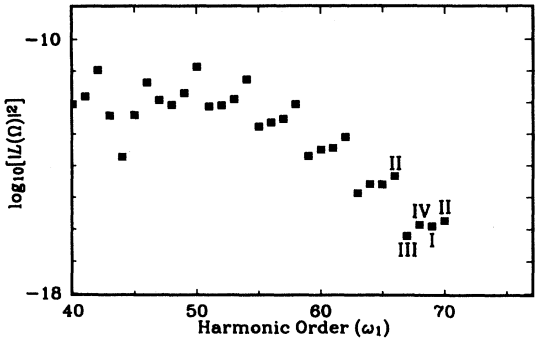

FIG. 9. $\log_{10}|L(\Omega)|^2$ vs harmonic order, $\omega_2 = 2\omega_1$, $|E_0| = 16.82\omega_1$, $\eta_2 = 5.0$, $\eta_1 = 0.5$, $\delta_1 = \delta_2 = 0$, $\epsilon_1 \cdot \epsilon_2 = 0.1$ (84°).

tracted from Eq. (2.34) or just be written down by inspection keeping in mind that the total number of photons absorbed from both fields must be odd. For $\omega_2 = 2\omega_1$ there are four different classes of harmonics based on their behavior when $\eta_1 \ll 1$, $\eta_1 \ll \eta_2$: type-I harmonics with frequencies $\Omega = (4m+1)\omega_1$, type-II harmonics with $\Omega = (2m+1)2\omega_1$, type-III harmonics with frequencies $\Omega = (4m-1)\omega_1$, and type-IV harmonics with frequencies $\Omega = 4m\omega_1$. Figure 8 shows the dependence of the intensities of the four different types of harmonics on the intensity of the low-frequency field when the high-frequency field is strong. Type-II harmonics go over to the one-color, strong field only, case as the weak field goes to zero. Type-IV harmonics are the even harmonics of the strong (ω_1) field. They vanish when the weak field goes to zero. At least two weak-field photons are required to generate a type-IV harmonic photon. Type-I and type-III harmonics are the odd harmonics of the weak field. They require at least one weak-field photon. They differ in the behavior of the term that is lowest order in the weak field, type-I harmonics take $2m$ photons from the strong field and *emit* one weak field photon, type-III harmonics take $2m$ photons from the strong field and *take* one photon from the weak field. Each type-IV harmonic is bracketed by a type-I and a type-III harmonic both with the same value of m_2. Since these two odd harmonic processes are of the same order in both fields it is not surprising that their magnitudes are similar. See, for instance, the $51\omega_1$ and $53\omega_1$ harmonics in Fig. 7 or Fig. 8. Table I summarizes the frequencies of the four types of harmonics and lists the photon numbers of the lowest-order processes for the weak, low-frequency field case. The power law relationships are also shown for the case where $\eta_1 \ll \eta_2 \ll 1$. The η_2 power laws fail when the high-frequency field strength increases, $\eta_2 \gtrsim 1$. However the η_1 power laws hold even when $\eta_2 \geq 1$ as long as $\eta_1 \ll 1$. If η_2 is turned down so that $\eta_2 < \eta_1$ then the weak field is the high-frequency field and a new set of lowest-order processes dominate. The lowest-order channels and power laws for the weak, high frequency field case are summarized in Table II. In this case there are only two types of harmonics, the odd harmonics which remain as the one-color harmonics when the second field is turned off, and the even harmonics which require at least one high-frequency photon.

We have already seen that the characteristics of the harmonics change rapidly as the angle between the polarization vectors approaches perpendicularity. Figure 9 shows the harmonic spectrum for the same field parameters as Fig. 7 except that the angle between the polarizations has been adjusted so $\epsilon_1 \cdot \epsilon_2 = 0.1$. This small change from perpendicular has a dramatic affect on the spectrum. In the falloff region the perpendicular harmonics in Fig. 7 show a characteristic pattern. The intensities of the odd, type-I and type-III harmonics are an order of magnitude or more below the intensities of the even, type-IV harmonic between them (for example the 63rd and 65th harmonics are below the 64th). When the angle between the fields is changed by just 6° the intensity of the type-I and type-III harmonics has risen to the same

TABLE II. Frequencies and scaling laws for the lowest order channels when $\omega_2 = 2\omega_1$, $\eta_2 \ll \eta_1 \ll 1$.

Type	Frequency	ω_1 photons	ω_2 photons	Power law
I, III	$\Omega = (2m+1)\omega_2$	$2m+1$	0	η_1^{2m+1}
II, IV	$\Omega = (2m)\omega_2$	$2(m-1)$	1	$\eta_2\eta_1^{2(m-1)}$
		$2(m+1)$	-1	$\eta_2\eta_1^{2(m+1)}$

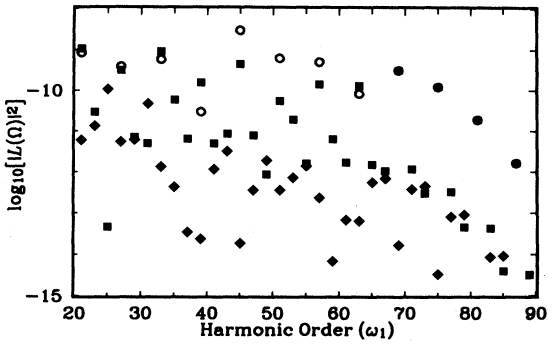

FIG. 10. The components of $L(\Omega)$ polarized in the ϵ_1 (squares) and the ϵ_2 (diamonds) directions from two linear, perpendicular fields, $\omega_2=3\omega_1$, $|E_0|=20.88\omega_1$, $\eta_1=5.0$, $\eta_2=0.5$, $\delta_1=\delta_2=0$. The open circles are the one-color spectrum of field 2 alone.

level as the intensity of the neighboring type-IV harmonic. Figure 9 is in much better agreement with the experimental results of Perry and Crane [9] than Fig. 7 which was calculated for the case of exactly perpendicular fields.

D. Commensurate frequencies ($\omega_2=3\omega_1$)

Above, in connection with Eq. (2.28), it was discussed that for two perpendicular linearly polarized driving fields the ϵ_1 and ϵ_2 series in Eq. (2.27) overlap whenever the ratio of the two frequencies equals the ratio of two odd integers. If this is the case then harmonics with arbitrary polarization, in particular circular polarization, can be generated, in principle, out of two perpendicular linearly polarized driving fields. Figure 10 shows the components of $L(\Omega)$ along both unit vectors for perpendicular fields with frequencies $\omega_2=3\omega_1$ and for $\delta=0$. For most of the harmonics one of the components dominates and the polarization is essentially linear, regardless of the phase of the other component. However, some of the harmonics have components with similar magnitudes. In particular the ϵ_1 and ϵ_2 components of the 27th and 55th harmonics are nearly identical in magnitude. The components of the 27th harmonic are nearly in phase, therefore its polarization is almost linear. However, Fig. 11 shows that the phase of the ϵ_2 component of the 55th harmonic leads that of the ϵ_1 component by 0.83π. The 55th harmonic is therefore, elliptically polarized. It should be kept in mind that there are various parameters that can be varied in order to achieve exactly the same magnitude for the two components. We reserve judgment here as to whether or not this is a practical way to generate harmonics with a specific polarization. The polarization will be critically dependent on the parameters of the driving field. Small changes in the intensities, phases, or polarization angles of the driving fields may affect the polarizations of the harmonics dramatically. In the laboratory these parameters are not constant in time or space and this will affect the quality of the polarization of the harmonics.

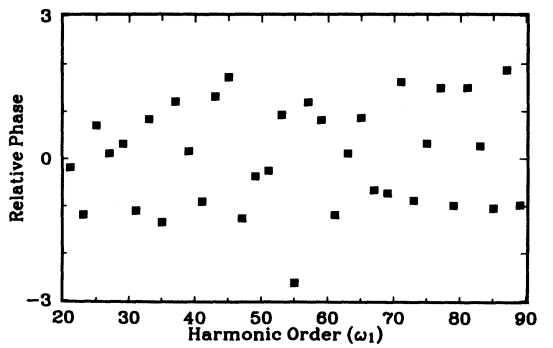

FIG. 11. The relative phase between the 1-component and the 2-components of $L(\Omega)$ for the conditions of Fig. 10.

IV. CONCLUSIONS

We have, in this paper, extended the δ-function potential model in order to calculate the properties of high-harmonic emission due to a superposition of two monochromatic driving fields for various polarization configurations. The justification for using such a highly simplified model atom is the growing conviction that many of the properties of the harmonics are governed by the propagation of the freed electron in the continuum subject to the driving fields rather than by the structure of the atom. We have been able to compare our results with two recent measurements [9,10] and found good agreement, given that we only compared the single-atom spectra and used plane-wave fields in the calculation and that the intensities of the experiments are not very well known. At this point we are tempted to draw the conclusion that results derived from this model can provide a useful guide to future experiments. The comparison with the data thus far available [9,10] has already taught some valuable lessons. For example, in the superposition of circularly polarized driving fields small deviations from perfect circular polarization may have a dramatic effect on the observed spectrum. Similarly, for linearly polarized driving fields, small deviations from perfect perpendicularity may completely alter the spectrum. Equally important, for commensurate frequencies variation of the relative phase can easily affect the intensity ratio of nearby harmonics by two orders of magnitude. These effects are likely to make the interpretation of experimentally observed spectra very tricky, in addition to the collective effects which are understood in principle, but nevertheless not easy to identify in practice. On the other hand, the single-atom polarization and phase effects offer great

potential for coherent control of high-harmonic emission. We have discussed the possibility of generating elliptic and circular polarization by perpendicular linearly polarized driving fields with a frequency ratio of 3:1 [or, more generally, (odd):(odd)]. However, if circular polarization is the goal, then it is easier to generate it via two circularly polarized incident beams such that the fields rotate in the same plane. We have not attempted to generalize the semiclassical model of the electron revisiting the core to a more than one-dimensional situation.

ACKNOWLEDGMENTS

We had fruitful discussions with B. Chichkov, H. Eichmann, M. Kleber, A. Lohr, and B. Wellegehausen. W.B. appreciates the hospitality of the theory division of the Physics Department of the Technical University of Munich as well as the Institute for Quantum Optics of the University of Hanover. W.B. also acknowledges partial support by the Sonderforschungsbereich SFB 338 of the Deutsche Forschungsgemeinschaft.

[1] A. McPherson, G. Gibson, H. Jara, U. Johann, T. S. Luk, I. A. McIntyre, K. Boyer, and C. K. Rhodes, J. Opt. Soc. Am. B **4**, 595 (1987); M. Ferray, A. L'Huillier, X. F. Li, L. A. Lompré, G. Mainfray, and C. Manus, J. Phys. B **21**, L31 (1988); X. F. Li, A. L'Huillier, M. Ferray, L. A. Lompré, and G. Mainfray, Phys. Rev. A **39**, 5751 (1989).

[2] A. L'Huillier, Ph. Balcou, S. Candel, K. J. Schafer, and K. C. Kulander, Phys. Rev. A **46**, 2778 (1992); A. L'Huillier, L. A. Lompré, G. Mainfray, and C. Manus, in *Atoms in Intense Fields, Advances in Atomic, Molecular, and Optical Physics, Supplement,* edited by M. Gavrila (Academic, London, 1992), p. 139.

[3] J. L. Krause, K. J. Schafer, and K. C. Kulander, Phys. Rev. A **45**, 4998 (1992); K. C. Kulander, K. J. Schafer, and J. L. Krause, in *Atoms in Intense Fields, Advances in Atomic, Molecular, and Optical Physics, Supplement,* edited by M. Gavrila (Academic, London, 1992), p. 247.

[4] K. C. Kulander, K. J. Schafer, and J. L. Krause, Phys. Rev. Lett. **68**, 3535 (1992).

[5] P. B. Corkum, Phys. Rev. Lett. **71**, 1994 (1993); P. Dietrich, N. H. Burnett, M. Ivanov, and P. B. Corkum, Phys. Rev. A **50**, R3585 (1994).

[6] K. S. Budil, P. Salières, A. L'Huillier, T. Ditmire, and M. D. Perry, Phys. Rev. A **48**, R3437 (1993).

[7] Y. Liang, M. V. Ammosov, and S. L. Chin, J. Phys. B **27**, 1269 (1994).

[8] F. A. Weihe, S. K. Dutta, G. Korn, D. Du, P. H. Bucksbaum, and P. L. Shkolnikov, Phys. Rev. A **51**, 3433 (1995).

[9] M. D. Perry and J. K. Crane, Phys. Rev. A **48**, R4051 (1993).

[10] H. Eichmann, A. Egbert, S. Nolte, C. Momma, B. Wellegehausen, W. Becker, S. Long, and J. K. McIver, Phys. Rev. A **51**, R3414 (1995).

[11] S. Watanabe, K. Kondo, Y. Nabekawa, A. Sagisaka, and Y. Kobayashi, Phys. Rev. Lett. **73**, 2692 (1994).

[12] M. Protopapas, P. L. Knight, and K. Burnett, Phys. Rev. A **49**, 1945 (1994).

[13] M. Shapiro, J. W. Hepburn, and B. Brumer, Chem. Phys. Lett. **149**, 451 (1988); S. M. Park, Sh.-P. Lu, and R. J. Gordon, J. Chem. Phys. **94**, 8622 (1991).

[14] C. Chen and D. S. Elliot, Phys. Rev. Lett. **65**, 1737 (1990).

[15] W. Becker, A. Lohr, and M. Kleber, Quantum Semiclass. Opt. **7**, 423 (1995).

[16] F. Ehlotzky, Opt. Commun. **13**, 1 (1975); L. C. M. Miranda, Phys. Lett. **86A**, 363 (1981); P. Stehle, Phys. Rev. A **26**, 2711 (1982); E. Fiordilino and M. H. Mittleman, *ibid.* **28**, 229 (1983); M. Ya. Agre and L. P. Rapoport, Zh. Eksp. Teor. Fiz. **90**, 1154 (1986) [Sov. Phys. JETP **63**, 672 (1986)]; C. Leone, S. Bivona, R. Burlon, and G. Ferrante, Phys. Rev. A **38**, 5642 (1988); P. Kálmán, Phys. Rev. **38**, 5458 (1988); M. Dörr and R. Shakeshaft, Phys. Rev. A **40**, 459 (1989); K. Rzążewski, L. Wang, and J. W. Haus, *ibid.* **40**, 3453 (1989); L. A. Bloomfield, Phys. Rev. Lett. **63**, 1578 (1989); J. Opt. Soc. Am. B **7**, 472 (1990); W. Becker, Li-E Li, and J. K. McIver, J. Phys. B **23**, L753 (1990); M. Pont and R. Shakeshaft, Phys. Rev. A **43**, 7856 (1991); L. Roso-Franco, K. Rzążewski, and J. H. Eberly, J. Mod. Opt. **38**, 997 (1991); F. Zhou and L. Rosenberg, Phys. Rev. A **44**, 3270 (1991); M. Dörr, R. M. Potvliege, D. Proulx, and R. Shakeshaft, *ibid.* **44**, 574 (1991); **45**, 2142 (1992); A. Bugacov, B. Piraux, M. Pont, and R. Shakeshaft, *ibid.* **45**, 3041 (1992); J. L. Madajczyk, M. Pont, R. M. Potvliege, R. Shakeshaft, and H. S. Taylor, *ibid.* **45**, 4848 (1992); C. M. Bowden, S. D. Pethel, C. C. Sung, and J. C. Englund, *ibid.* **46**, 597 (1992); S. Bivona, R. Burlon, G. Ferrante, and C. Leone, *ibid.* **50**, R1984 (1994).

[17] A. Szöke, K. C. Kulander, and J. N. Bardsley, J. Phys. B **24**, 3165 (1991); R. M. Potvliege and P. H. G. Smith, *ibid.* **24**, L641 (1991); **25**, 2501 (1992); K. J. Schafer and K. C. Kulander, Phys. Rev. A **45**, 8026 (1992); N. B. Baranova, H. R. Reiss, and B. Ya. Zel'dovich, *ibid.* **48**, 1497 (1993); R. M. Potvliege and P. H. G. Smith, *ibid.* **49**, 3110 (1994); V. A. Pazdzersky and V. A. Yurovsky, *ibid.* **51**, 632 (1995).

[18] A. M. Perelomov and V. S. Popov, Zh. Eksp. Teor. Fiz. **52**, 514 (1967) [Sov. Phys. JETP **25**, 336 (1967)]; M. Elk, P. Lambropoulos, and X. Tang, Phys. Rev. A **44**, R31 (1991).

[19] M. D. Davidson, J. Wals, H. G. Muller, and H. B. van Linden van den Heuvell, Phys. Rev. Lett. **71**, 2192 (1993).

[20] H. G. Muller, H. B. van Linden van den Heuvell, and M. J. van der Wiel, J. Phys. B **19**, L733 (1986); H. G. Muller, P. H. Bucksbaum, D. W. Schumacher, and A. Zavriyev, *ibid.* **23**, 2761 (1990); H. G. Muller, Comments At. Mol. Phys. **24**, 355 (1990).

[21] W. Becker, S. Long, and J. K. McIver, Phys. Rev. A **41**, 4112 (1990); **46**, R5334 (1992).

[22] W. Becker, S. Long, and J. K. McIver, Phys. Rev. A **50**, 1540 (1994); this paper will hereafter be referred to as I.

[23] A. L'Huillier, M. Lewenstein, P. Salières, Ph. Balcou, M. Yu. Ivanov, J. Larsson, and C. G. Wahlström, Phys. Rev. **48**, R3433 (1993); M. Lewenstein, Ph. Balcou, M. Yu. Ivanov, A. L'Huillier, and P. B. Corkum, Phys. Rev. A **49**, 2117 (1994).

[24] J. J. Macklin, J. D. Kmetec, and C. L. Gordon III, Phys. Rev. Lett. **70**, 766 (1993).

[25] K. Miyazaki and H. Sakai, J. Phys. B **25**, L83 (1992); K. Kubodera, Y. Nagata, Y. Akiyama, K. Midorikawa, M. Obara, H. Tashiro, and K. Toyoda, Phys. Rev. A **48**, 4576 (1993).

[26] K. Kondo, T. Tamida, Y. Nabekawa, and S. Watanabe, Phys. Rev. A **49**, 3881 (1994).